INTERNATIONAL JOURNAL OF OPTIMIZATION IN CIVIL ENGINEERING
Int. J. Optim. Civil Eng., 2022; 12(3):365-398

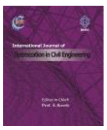

AN EFFECTIVE HYBRID METHOD FOR OPTIMIZING STEEL FRAMES WITH IMPROVED SEISMIC PERFORMANCE

R. Bagherzadeh, A. Riahi Nouri, M. S. Massoudi[*, †], M. Ghazi and F. Haddad Sharg
Department of Civil Engineering, West Tehran Branch, Islamic Azad University, Tehran, Iran

ABSTRACT

The main purpose of this paper was to use a combination of Energy-based design method and whale algorithm (WOA), hereinafter referred to as E-WOA, to optimize steel moment frames and improve the seismic performance. In E-WOA, by properly estimating the seismic input energy and determining the optimal mechanism for the structure, steel frames are designed based on the energy balance method; according to the results, in a suitable search space, optimization is performed using the WOA algorithm. The objective function of the WOA algorithm, in addition to the frame weight, is meant to improve the behavior of the structure based on the performance level criteria of the ASCE41-17 standard and the uniformity of the drift distribution at the frame height. The results show that the initial design of the Energy method reduces the computational volume of the WOA algorithm to achieve the optimal solution and the plastic hinge pattern in frame is more favorable in the E-WOA method than in the design done by the Energy method.

Keywords: energy-based design methods; whale algorithm; optimization of steel moment frame; lateral loading pattern; nonlinear static analysis.

Received: 5 February 2022; Accepted: 15 April 2022

1. INTRODUCTION

Standard codes and building design standards are basically founded on linear static analysis with the application of coefficients to predict the nonlinear behavior of the structure. Function-based design methods and seismic codes impose stricter conditions for

[*]Corresponding author: Department of Civil Engineering, West Tehran Branch, Islamic Azad University, Tehran, Iran
[†]E-mail address: Massoudi.ms@wtiau.ac.ir (M. S. Massoudi)

deformations. Compared to methods that are mainly based on resistance, these methods show the behavior of the structure in more detail in the face of lateral displacements caused by earthquakes. In contrast, performance-based design is not necessarily reliable and cannot meet structural requirements in terms of resistance. Therefore, developing methods that can create a proper balance between strength and seismic performance of the structure is one of the main needs of structural designers and engineers. Among structural design methods, Energy-based methods used for designing structures can be much more explicit and realistic than other methods. These methods are based on the balance of the input and output energy of structures; so, in their equations, in addition to using the earthquake peak point, the effects of other characteristics of an earthquake and deformation concepts can be applied simultaneously [1]. Energy-based design methods can also be effective in discussing the search for damage points in structures. Housner (1956) [1], for the first time, proposed a method for the Energy-based design; since then, many researchers have used these methods [2-17].

Important earthquakes in 1989 (Loma Prieta, USA), 1994 (Northridge, USA) and 1995 (Kobe, Japan) marked a turning point in the evolution of earthquake engineering. The idea of performance-based earthquake engineering was introduced at this time [18]. According to this method, structures are designed for their performance in order to design economically optimal structures and minimize the loss of life and property in important and crowded buildings [18]. In defining the design based on the performance of buildings, performance is divided into three levels: immediate occupancy (IO), life safety (LS) and collapse prevention (CP) [19]. Fig. 1 shows the structure's push graph with a graphical representation of the amount of damage at different functional levels of the building.

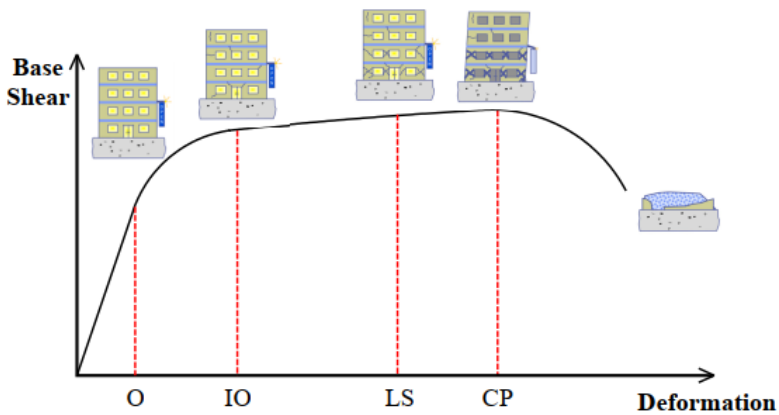

Figure 1. Base shear-deformation diagram of the structure with different functional criteria [20]

In regard to simultaneously meeting the strength needs and the seismic performance of the structure, relationships and equations can be sometimes difficult and thus, unsolvable; these can be solved through approximate methods such as trial and error Optimization with meta-heuristic methods is one of such methods. In the recent years, many meta-heuristic methods such as genetic algorithm (GA) have been developed [21].

Harmony Search (HS) [22], Ant Colony Optimization (ACO) [23], Artificial Bee Colony

(ABC) [24], Particle Swarm Optimization (PSO) [25], Imperial Competitive Algorithm (ICA) [26,27], Firefly algorithm (FA) [28], Bat algorithm (BA) [29] and Dolphin algorithm (DE) [30] have been widely used. An efficient optimization method was recently proposed by Mashayekhi et al. [31] which was a combination of Imperialist Competitive Algorithm (ICA) and Gravitational Search Algorithm (GSA). Furthermore, to achieve Reliability-Based Topology Optimization (RBTO) of double layer grids, Mashayekhi et al. [32] have introduced SIMP-ACO method.

In the recent years, various studies have been conducted to investigate the optimization of steel moment frames using meta-heuristic methods. Fragiadakis et al. (2006) [33], proposed an evolutionary strategies-based method for the optimal design according to the performance of steel structures, by taking into account the inelastic behavior of the structure [33]. Talatahari (2013) also optimized the steel moment frame using PSO and PSASD algorithms based on the base shear criterion [34].

Further, Kaveh and Nasrollahi (2014) applied a similar method by using the CSS algorithm to optimize moment frames [35]. Gholizadeh and Poorhoseini (2015) also proposed a combination of neural networks and a modified firefly algorithm for size optimization based on the performance of steel frames [36].In addition, Karimi and Vaez (2019) presented a two-step method to remove the limitations of ductility and resistance control [37]. Gholizadeh et al (2020) also proposed a combination of neural networks and a modified firefly algorithm for size optimization based on the performance of steel frames [38].Similarly, Degertekin et al (2021) recently proposed a metaheuristic method called school-based optimization (SBO) in the performance-based optimum seismic design of steel frames [39].

Much work has been done on the design and optimization of buildings based on performance criteria. In 2002, Hassan et al. [40], for instance, used the idea of rigid hinges and target displacement presented in FEMA 273 to discuss performance-based seismic design. In 2006, Grierson et al. [41], also used classical algorithms to optimize moment frames, considering the shear criterion as the constraint and weight of the structure along with the inelastic ductility capacity as the objective function. In 2008, Salajegheh et al. [42], also used the FEMA356 standard to control the rotation and displacement of the target structure to optimize X-braced frames.On the other hand, in 2010, Kaveh et al. [43], optimized the weight of a steel moment frame using a performance-based design method and the Ant Colony Algorithm (ACO). In 2011, Tehranizadeh and Musharaf [44], also optimized moment frames using IDA analysis, in which the objective function was the weight of the structure and the maximum energy lost in the structural system. In 2013, 2015, 2020 Gholizadeh optimized the structures using a meta-heuristic algorithm [45, 46 and 38].

The main purpose of this paper is to use Energy-based design method and integrate its results with the Whale Algorithm (WOA) in the optimization of steel moment frames. In the Energy method, the design of the members is based on equalizing the difference between the input energy of the structure and the elastic energy absorbed in the structure with the energy dissipated in the plastic hinges. In relation to equilibrium, the effect of gravitational loads and higher modes on the energy entering the structure and the impact of the decrease in the resistance of the members in the cyclic forces on the energy dissipated in the plastic hinge have been investigated. The dissipated energy of the system is the result of the energy

wasted in each of the plastic hinge formed on the frame. Based on this balance, the minimum required momentum of the beams will be obtained; through this, the beams and columns will be designed based on constraints such as strong-column weak-beam, and soft and weak stories.

The Whale Algorithm (WOA) has also been used to improve the results of the Energy method. In the first stage, based on the performance level of OP and CP, according to ASCE41-17 [47], the allowable displacement of the Energy method is determined and the design results are obtained based on both performance levels. In the second step, the WOA algorithm searches for the optimal position within the range of the results of these two levels. After obtaining the results of the methods, the E-WOA method (combination of WOA algorithm and Energy method), finally uses the nonlinear static analysis to control the results. The study models in this paper are three 8, 16, and 24-story moment frames that are in a regular height. The drift of stories and the deformation of beams are controlled according to AISC2016 codes [48]. At this stage, the structural needs are controlled based on the limit state method. Push-over analysis begins with constant gravitational loads and incremental lateral loads. In this case, the structure is subjected to nonlinear push-over analysis with a uniform distribution and controlled for four functional levels in the target displacement. The control criteria for this stage are taken from ASCE41-17 [47]. All codes are performed in MATLAB [49], and static linear and nonlinear modeling and analysis are performed using SAP2000 software [50].

2. ENERGY-BASED DESIGN METHOD IN STEEL FRAMES

The concept of energy based design method in steel frames is based on the assumption that the amount of energy required to push a structure in a one-way load to reach the target displacement is equal to the maximum input energy of the earthquake, which is approximated by $\frac{1}{2}\gamma M \times S_v^2$ [50]. For multi-degree-of-freedom systems, all vibration frequencies or structural alternation periods are effective in calculating the seismic input energy that is full of different frequency components [51]. The input energy of multi-degree-of-freedom systems can be written according to Equation (1) [51]:

$$E = \sum_{n=1}^{N} \Gamma_n^2 . E_{SDOF,n} \tag{1}$$

Γ_n, the modal participation factor for the Mode n is calculated from Equation (2):

$$\Gamma_n = \frac{L_n}{M_n^*} \qquad L_n = \phi_n^T M l \qquad M_n^* = \phi_n^T M \phi_n \tag{2}$$

ϕ_n is the vector of the eigenvalues and M is the mass matrix. According to the following equation, the input energy of a system is calculated as one degree of freedom, $E_{SDOF,n}$ [51].

$$E_{SDOF,n} = \frac{1}{2} M_n^* V_{MAX,n}^2 = \frac{1}{2} M_n^* S_{v,n}^2 = \frac{T_n^2}{8\pi^2} M_n^* S_{a,n}^2 \tag{3}$$

where $S_{v,n}$ and $S_{a,n}$ are the spectral velocity and the spectral acceleration of each mode obtained from the elastic response spectrum; T_n is the period of the nth mode. In dissipation systems with a decreasing behavior in deformation cycles, there are major cycles that control the input energy of these systems.

Akiyama (1985) [53] showed that the elastic energy for a single-degree-of-freedom (SDOF) could be written as Equation (4) with acceptable accuracy:

$$E_e = \frac{1}{2} V_y \Delta_y = \frac{1}{2} M \left(\frac{T_e}{2\pi} . \frac{V_y}{W} g \right) \tag{4}$$

where V_y is the base shear yield, Δ_y is the yield displacement limit and T_e is the period of the structure, g is the gravitational acceleration and W is the weight of the structure.

The frame's yield mechanism is assumed as shown in Fig. 2. Plastic deformation of the frame occurs after the structure reaches the yield point.

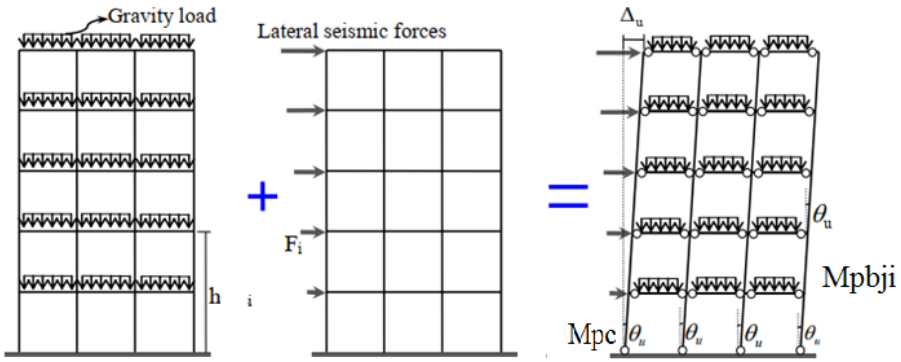

Figure 2. How a frame's yield mechanism [51]

According to the Hazner's assumption, the energy entering the structure is equal to the sum of elastic and plastic energy [2]. According to Equation (5), Leelataviwat et al. (1999) [52] proposed an Energy-based approach to the performance-based design in which the need for drift control was eliminated at the end of the design. The concept of energy balance is

shown in Fig. 3.

$$E_e + \eta E_p = \lambda E \tag{5}$$

where E is the input energy to the structure, E_e is the elastic energy and E_p is the energy dissipated by plastic hinges. λ and η are the damping coefficients and the behavior of the curve representing the deformation cycle of the structure, respectively.

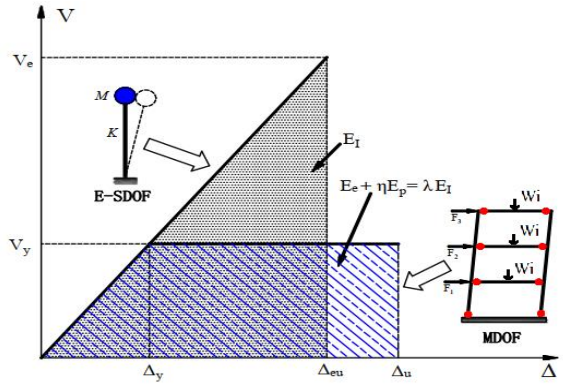

Figure 3. The concept of energy balance [52]

The value λ was considered equal to $\lambda = 1/(1+3\xi+1.2\sqrt{\xi})^2$ by Akiyama 1985 [53];in ξ is the damping of the structure. To define η , the effects of earthquake reciprocating behavior on sections can be seen in references [51].

According to Equations (1, 4 and 5), the total plastic energy a structure must dissipate during an earthquake for a system with multi degrees of freedom is equal to:

$$E_P = \frac{\lambda E - E_e}{\eta} = \left(\lambda . \sum_{n=1}^{N} \Gamma_n^2 . (\frac{T_n^2}{8\pi} M_n^* S_{a,n}^2) - \frac{1}{2} M . \left(\frac{T_e}{2\pi} . \frac{V_y}{W} g \right)^2 \right) . \eta^{-1} \tag{6}$$

The rotation related to the plastic area of the frame (θ_p) will be equal to the difference between the total elastic and plastic rotation of the frame and elastic rotation. In this paper, nonlinear static analysis is performed to accurately determine θ_p . Also, the rotation of a point on the curve whose slope changes is considered as the value of the elastic rotation.

The energy obtained from Equation (6) must be dissipated by the plastic hinges shown in Fig. 1, which is equal to:

$$E_P = \left((m+1) M_{pc} + 2 \sum_{j=1}^{m} \mu_j \sum_{i=1}^{n} \beta_i M_{pbr} \right) \theta_p \tag{7}$$

where M_{pbr} is the reference moment of the plastic beam at the j[th] opening, M_{pc} is the plastic moment of the base of the columns on the first story, m is the number of frame openings, n is the number of frame stories and β_i is the coefficient of the resistance distribution of the beams (the value of which is mentioned below) on the 1[st] story. Also, $\mu_j = \frac{l_r}{l_j}$ is the reference moment coefficient of the beams, which is equal to the ratio of the length of the reference opening (such ,a larger aperture) to the length of the j[th] opening.

In addition, after yield, external forces must be in balance with the internal ones. By equating the energy dissipated in the plastic state with the external work done by lateral forces and gravitational loads, we can act according to Equation (8):

$$E_P = V_y \left(\frac{\sum_{i=1}^{n} W_i h_i^{k+1}}{\sum_{i=1}^{n} W_i h_i^{k}} \right) \theta_p + \sum_{i=1}^{n} W_i \frac{\theta_p{}^2 h_i}{2} \tag{8}$$

In order to obtain the base shear of the frame with a suitable estimation, the input energy of the dissipated earthquake by (Equation 6) can be equal to the work done by external forces (on plastic hinge), which includes lateral and gravitational loads according to Equation (9).

$$V_y \left(\frac{\sum_{i=1}^{n} W_i h_i^{k+1}}{\sum_{i=1}^{n} W_i h_i^{k}} \right) \theta_p + \sum_{i=1}^{n} W_i \frac{\theta_p{}^2 h_i}{2} = \left(\lambda . \sum_{n=1}^{N} \Gamma_n^2 . (\frac{T_n^2}{8\pi} M_n^* S_{a,n}^2) - \frac{1}{2} M . \left(\frac{T_e}{2\pi} . \frac{V_y}{W} g \right)^2 \right) . \eta^{-1} \tag{9}$$

where K is equal to:

$$\begin{aligned} & K = 0.5T + 0.75 \\ & if \quad T \le 0.5 \rightarrow k = 1 \\ & if \quad T \ge 2.5 \rightarrow k = 2 \end{aligned} \tag{10}$$

By solving the quadratic equation of Equation (9), the base shear value will be obtained. Once the base shear is determined, the design force of each level is obtained.

To calculate the beam's M_{pbr}, the plastic moment of the columns, M_{pc}, must be properly estimated. This appropriate value is obtained by using the assumption of preventing the formation of soft story failure in the first story. For this purpose, plastic hinges at the top

and bottom of the first floor columns are assumed. The plastic moment capacity of the floor columns is determined to prevent the formation of this failure state using Fig. 4.

$$M_{pc} = 1.1\left(\frac{V_y h_1 + W h_1 \theta_p}{2(m+1)}\right) \tag{11}$$

The parameters of this relation have been introduced before.

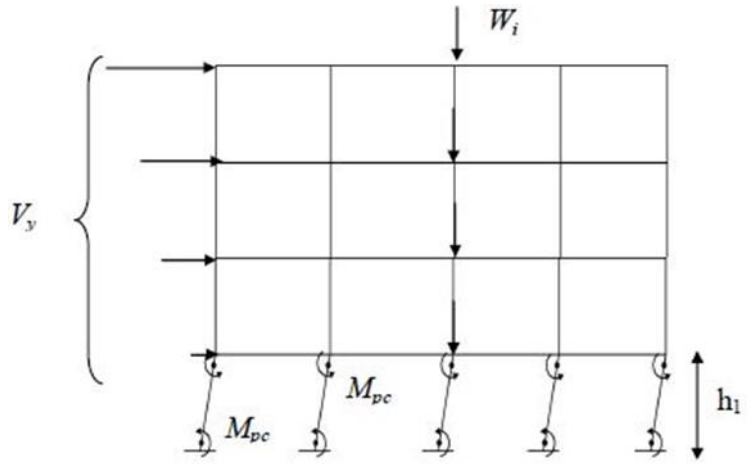

Figure 4. Soft story failure mode

The coefficient of resistance distribution, β_i, plays a very important role in the seismic response of structures. This coefficient depends on the hardness and lateral strength of the structure along the height. β_i must be properly selected to match the forces exerted during the earthquake. It also ensures that the incoming energy is dissipated in the structure, preventing damage from being concentrated on one floor. Numerous numerical analyses were performed to obtain the best resistance distribution of the beams. The aim was to obtain a function that could well express the shear resulting from different earthquakes. As an initial approximation, the relative distribution of stories shear during an earthquake can be approximated by the distribution of stories static shear, as calculated from (12). Its value is equal to [52]:

$$\beta_j = \left(\frac{V_i}{V_y}\right)^{1/2} \tag{12}$$

where V_i and V_y are static shear in the ith level and the level of the highest floor, respectively. The value of 1/2 is obtained using the least squares method from the results

obtained from several nonlinear dynamic analyses [52]. By establishing the equation of relations (7) and (8) and knowing its unknowns, the value of M_{pbr} is obtained; then, through that value, the design moment of the beams is calculated as follows:

$$\varphi M_{pbij} \geq \mu_j \beta_i M_{pbr} \tag{13}$$

where φ is the resistance coefficient; according to AISC2016 [48], it is equal to 0.9. M_{pbij} is the plastic moment of the beam in the ith floor and the jth opening.

3. WHALE OPTIMIZATION ALGORITHM (WOA)

The WOA algorithm is based on the collective intelligence of humpback whales and the strategy of hunting by a ring of bubbles; it was first proposed by Mirjalili and Laviz [54]. Whales have cells similar to human spinal cord cells in certain areas of their brains [55]. Whales have, however, more of these cells than adults, which is the main reason for their intelligence. It has been proved that the whale can think, learn, judge, communicate and even become emotional like a human, though obviously with a much lower level of intelligence. The WOA method involves three operators, including bait search simulation, bait siege, and humpback whale bubble nets [55].

(A) Siege of prey

This behavior is represented by relationships (14 and 15) [54]:

$$\vec{D} = \left| \vec{C}.\vec{X}^{*}(t) - \vec{X}(t) \right| \tag{14}$$

$$\vec{X}(t+1) = \vec{X}^{*}(t+1) - \vec{A}.\vec{D} \tag{15}$$

where t is the iterations counter, $\vec{A}$ and $\vec{C}$ are constant coefficients, and X^{*} is the position vector of the best solution ever obtained, and $\vec{X}$ is the position vector; also | | t is an absolute value sign and represents multiplication. It should be noted here that X^{*} should be updated in each iteration if there is a better solution. The vectors are calculated according to Equations (16-17) [54].

$$\vec{A} = 2\vec{a}.\vec{r} - \vec{a} \tag{16}$$

$$\vec{C} = 2.\vec{r} \tag{17}$$

where a decreases linearly from 2 to 0 during iterations (in both exploration and exploitation stages) and r is a random vector in [0.1].

(B) Bubble whales (operation stage)

The mathematical model is described in relation (18) [54]:

$$\vec{X}(t+1)=\begin{cases}\vec{X}^{*}(t)-\vec{A}.\vec{D} & \text{if } p<0.5\\ \vec{D}'.e^{bl}.\cos(2\pi l)+\vec{X}^{*}(t) & \text{if } p\geq 0.5\end{cases} \tag{18}$$

where p is a random number in [0.1].

(C) Bait search (exploration stage)

This step of the algorithm is set to address the issue of exploration. Therefore, according to what is defined for the vector $\vec{A}$ in relation (18), if the random values of the vector $\vec{A}$ are greater than 1 and less than 1, the algorithm will move the whale to an area farther away from the position of the reference whale. Unlike the use step, the operation of the algorithm in this step is using random motion instead of moving to the superior samples, thus preventing the early convergence of the algorithm; in other words, by using the | |> 1 mechanism, general search mechanism is done. The mathematical model is in accordance with relations (19 and 20) [54]:

$$\vec{D}=\left|\vec{C}.\overrightarrow{X_{rand}}-\vec{X}\right| \tag{19}$$

$$\vec{X}(t+1)=\overrightarrow{X_{rand}}-\vec{A}.\vec{D} \tag{20}$$

$\overrightarrow{X_{rand}}$ is a random position vector (a random whale) selected from the current population. The pseudo-code of the WOA algorithm is presented in Fig. 5.

```
    Initialize the whales population Xi (i = 1, 2, ..., n)
Calculate the fitness of each search agent
X*=the best search agent
while (t < maximum number of iterations)
   for each search agent
    Update a, A, C, l, and p
     if1 (p<0.5)
          if2 (|A| < 1)
       Update the position of the current search agent by the Eq. (20)
          else if2 (|A|≥1)
        Select a random search agent ( )
        Update the position of the current search agent by the Eq. (23)
          end if2
    else if1 (p 0.5)
       Update the position of the current search by the Eq. (25)
    end if1
  end for
  Check if any search agent goes beyond the search space and amend it
  Calculate the fitness of each search agent
  Update X* if there is a better solution
  t=t+1
end while
return X*
```

Figure 5. Pseudo-code of the WOA algorithm [54]

The steps of the modified Whale Algorithm (E-WOA) are as follows:

1. Providing basic parameters of WOA algorithm and Energy method
   In this step, the variables are the cross-sectional area of the beams and columns. The list of profiles is made up of the W-shaped sections, which are arranged according to the size of the cross-sectional area.
2. Determining the search range of each variable in the WOA algorithm based on the Energy method
3. In this step, based on the list of the sections of the previous step and Energy method, with two different values for θ_p (the value of this period in the CP criterion for the lower limit of variables vector and the value of this rotation in the OP criterion for the upper limit of design variables), the design results are obtained and stored under the names $X_{UB,Energy}$ and $X_{LB,Energy,}$ respectively.
4. Calculating the values of 1, C, A and p in the WOA algorithm according to the reference [54].
5. Executing the Whale Algorithm (WOA) in the search space limited to $X_{UBEnergy}$ and $_{XLB\ Energy}$ vectors
6. Calculating the objective function and checking the convergence conditions; if it is not established, return to step 2.

4. NONLINEAR STATIC ANALYSIS

The finite element planar model of the above tree steel frames was established by the

software SAP2000 [61]. The finite element model is shown in Figs. 6, 7 (Take the 8-story steel frame as an example). The frame sections are adopted for all the beams and columns. Each beam and column comprises only one element with two nodes. The steel frames are all rigidly connected. The column base is fixed.

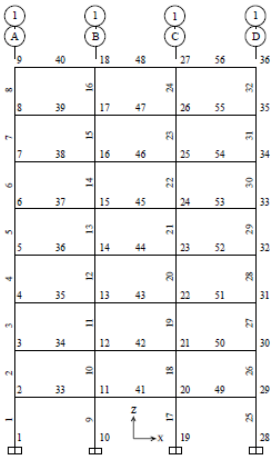

Figure 6. Finite element planar model of 8-story steel frame

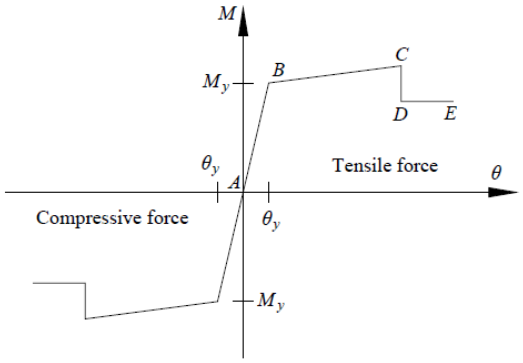

Figure 7. Constitutive relation of the hinge P-M-M

The finite element planar model was established completely and the corresponding pushover analyses were performed. The hinge P-M3 was used to simulate the material nonlinearity of the frame columns, and the hinge M3 was applied to simulate the nonlinearity of the frame beams. The constitutive relation of the hinge P-M-M is shown in Fig. 4. The vertical coordinate represents the bending moments and the horizontal coordinate indicates the rotation. The mechanical behavior of plastic hinges can be determined in accordance with ASCE41-17 [47]. During the pushover analysis, the material strength uses the average values, and the lateral force adopts the inverted triangular distribution pattern.

The push-over analysis, was done in accordance with ASCE41-17[47]. To apply the combination of gravity loads and lateral load distribution patterns, in the combination of gravity and lateral loads, the upper and lower limits of gravity load effects, Q_G ,were calculated from the relations (21 and 22).

$$Q_G = 1.1(Q_D + Q_L) \tag{21}$$

$$Q_G = 0.9Q_D \tag{22}$$

where Q_D and Q_L are the effective seismic dead and live loads, respectively.

According to Section 2, the frames are designed based on the Energy method, with OP and CP performance levels. Finally, a list of the sections of beams and columns for the two defined levels is obtained. In order to improve the results, the whale meta-heuristic algorithm (WOA) must look for the optimal solution for the structure in the interval between the two performance levels OP and CP.

Finally, totally three methods were used to compare the results in this study. Energy

methods and E-WOA, were two of these methods. In the section related to examples and numerical results , to compare the results, all two methods were analyzed and examined based on nonlinear static analysis.

5. MATHEMATICAL OPTIMIZATION PROBLEM

Despite the desirable characteristics of the Energy-based method, including the proper estimation of the frame sections without the need for trial and error, hypotheses and approximations considered in this method, including the initial assumption in calculating the input energy given to the structure, caused the results obtained by this method not to be compatible with the design objectives. On the other hand, in order to have control on goals such as design based on performance and some limitations such as deformation and resistance of members, drift of stories and, strong-column weak-beam, simultaneously and definitively, it is necessary to use optimization with meta-heuristic algorithms. Therefore, in this paper, the WOA algorithm and its combination with the Energy method have been used.

One of the main problems in optimizing frames in the nonlinear mode is the high computational volume and its time-consuming nature. In this article, by using the Energy method, the search space has been reduced in a suitable way, leading to a very good reduction in the volume of calculations.

The mathematical function of this problem, like any other optimization problem, has a goal, several constraints and variables, and the limits of each variable. For the nonlinear static method, the general relationship of the deformation force, as shown in Fig. 8, can be used. The effects of strain hardening are taken into account by considering a slope equal to 3% of the slope of the elastic part. Details of this figure are given in ASCE41-17 [47].

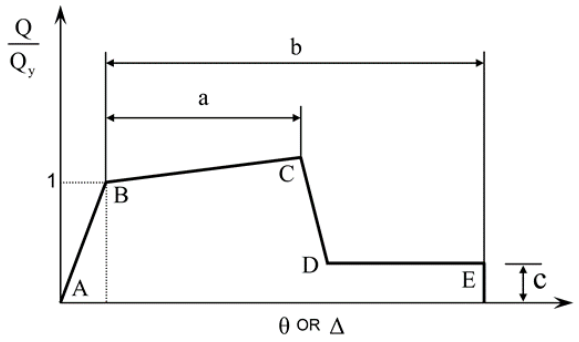

Figure 8. General force-deformation curve for members and components [47]

In most optimization problems, the main objective function of minimizing the weight of the structure and other design objectives are added to the problem as the constraints. In this study, the objective function, in addition to the weight of the structure, has been achieving the desired mechanism in which the maximum capacity of the structure is used. Finally, the relation of the objective function is as follows:

$$F(x) = w_1 \sum_{j=1}^{ne} W_{Lj} L_j \tag{23}$$

In this relation L_j is the member length and, W_{Lj} is the weight of the jth element.

In order to ensure the correct design, in addition to weight optimization, the performance and resistance parameters have been controlled according to the AISC2016 standards [48].

During the optimization process, target displacement of each candidate design is calculated using Eq. (24) to carry out the pushover analysis.

$$\delta_t = C_0 C_1 C_2 C_3 S_a \frac{T_e^{\,2}}{4\pi^2} g \tag{24}$$

where C_0, C_1, C_2, and C_3 factors are determined in accordance with ASCE41-17 [47]; The structural effective fundamental period is represented by T_e; the ground motion acceleration is represented by g; and S_a is the spectral acceleration; in this study, it is calculated in accordance with the ASCE41-17 code [47]. The analysis is based on the assumption that the amount of the displacement of the roof target is equal to 0.004, 0.007, 0.025 and 0.05, relative to the total height of the structure. Each of these represents the performance levels of OP, IO, LS and CP. The story drift is controlled for all functional levels, but the permissible rotation of the members is checked for the last three target movements.

After performing nonlinear analysis and obtaining the required results, the constraints are checked as follows:

Seismic constraints: For beams, based on the slenderness ratio, the constraint related to the rotation of the member is controlled by Equation (25).

$$\theta_{beam} \le \theta_{all}^{i} \qquad \text{i=OP,IO,LS,CP} \tag{25}$$

In this relation, θ_{all}^{i} is equivalent to the rotation of the beam at its end and θ_{beam} is the permissible displacement in ASCE41-17 [47] based on the desired level of performance.

For columns, based on the displacement of the control, the permissible rotation must be controlled by relation (26). Based on the control force, the control of the force ratio in the final stage of the analysis to the column capacity should be done according to Equation (27).

$$\theta_{column} \le \theta_{all}^{i} \qquad \text{i=OP,IO,LS,CP} \tag{26}$$

$$\frac{P_c}{\phi P_n} + \frac{M_c}{\phi M_n} \le 1 \tag{27}$$

In this relation, P_C and ϕP_n are the axial force and the nominal capacity of the column,

respectively. M_c and ϕM_n are also the present bending moment and the nominal capacity of the column, respectively. θ_{column} is also permissible displacement in ASCE41-17[47] based on the desired performance level.

Story drift constraint is controlled by relation (28):

$$\Delta^i_{\text{int}erstory} \le \Delta^i_{all\ \text{interstory}} \tag{28}$$

So $\Delta^i_{\text{interstory}}$ is the story drift based on the desired performance level and $\delta^i_{all\ \text{interstory}}$ is the allowable floor drift equal to 0.65, 0.31, 0.061, 0.012 in OP to CP performance levels [38, 40].

Strong column weak beam constraint is defined as relation (29):

$$\frac{\sum M_{P\ \text{column}}}{\sum M_{P\ \text{beam}}} \ge 1 \tag{29}$$

According to this relation, $M_{P\ \text{beam}}$, $M_{P\ \text{column}}$ refer to the plastic moment of the columns and beams, respectively.

Non-seismic constraints: The constructability requirements necessitates that the dimensions of beams and columns in all framing hinges be consistent. Therefore, geometric constraints should be checked in each framing hinges of SMFs as follows:

$$\left\{\left(\frac{b_B}{b_C^B}-1\le 0\right),\left(\frac{b_C^T}{b_C^B}-1\le 0\right),\left(\frac{h_C^T}{h_C^B}-1\le 0\right)\right\} \tag{30}$$

where b_B and b_c^B are the beams and columns flange width, b_C^B and b_C^T are the flange width of the bottom and top columns, respectively, and h_C^B and h_C^T are the depth of bottom and top columns, respectively. Furthermore, in order to ensure that the structural elements have sufficient strength against gravity non-seismic loads, the strength constraints should be checked in accordance with the AISC−LRFD [48] design code for each member of planar SMFs as follows:

$$\begin{cases} \dfrac{P_u}{2\phi_c P_n}+\dfrac{M_u}{\phi_b M_n}-1=0 & for\ \dfrac{P_u}{\phi_c P_n}<0.2 \\ \dfrac{P_u}{\phi_c P_n}+\dfrac{M_u}{\phi_b M_n}-1=0 & for\ \dfrac{P_u}{\phi_c P_n}\ge 0.2 \end{cases} \tag{31}$$

where P_u and P_n are the required and nominal axial strengths, respectively, ϕ_c and ϕ_b are resistance factors, and M_u and M_n are the required and nominal flexural strengths, respectively.

6. NUMERICAL EXAMPLES

To validate the WOA method presented in this paper, one well-known small-scale truss structure is used. The suggested truss is a benchmark example that has been widely used in the past [56];

In this example, for WOA algorithms, the maximum number of iterations (T) and the population size (NP) were considered as 1000 and 20, respectively. To assess the effect of the initial population on the final results, this example was solved 20 times using various sets of starting designs randomly generated, and some stochastic parameters were adopted for the purpose of comparison.

This model was the 10 bar plane truss shown in Fig. 9. The design variables were the cross-sectional areas of the ten elements, which were treated as continuous design variables. At each of the free nodes (2, 3, 5, and 6), a non-structural mass of m=453.6 kg (1000lb) was attached. The natural frequency constraints were $f_1 \geq 7$ Hz, $f_2 \geq 15$ Hz, and $f_3 \geq 20$ Hz. The minimum allowable area of the cross-sectional area was 6.45×10^{-5} m^2 (0.1 in^2).

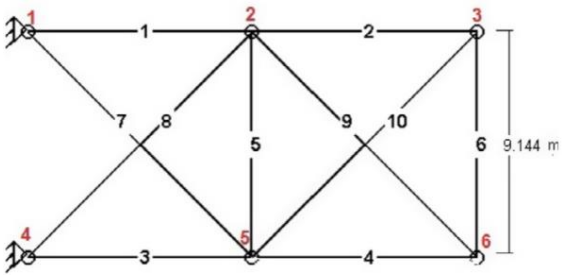

Figure 9. 10 bar plane truss*[56]*

The goal of truss optimization is to minimize the weight of the structure under such design constraints as natural frequency, element stresses, and nodal displacements. In this example, a combination of these types of truss optimization is employed for the minimization of the structural weight. Natural frequency, stress, displacement, and/or buckling constraints are imposed. Thus, the optimization problem can be posed as (32):

$$\begin{aligned} &\textit{Find}: A = [a_1, a_2, ..., a_{NMG}] \\ &\textit{to minimize:}\ \ W(A) = \sum_{k=1}^{NM} \rho_k a_k L_k + \sum_{j=1}^{nj} b_j \\ &\textit{subject to}: \quad g_f, g_\sigma, g_\lambda, g_\delta \leq 0 \end{aligned} \tag{32}$$

where the A vector includes the sizing variables (i.e., cross-sectional areas of bars), $W(\mathbf{A})$ is the weight of the truss structure, ρ_k and L_k, are the material density and length of the kth member, respectively, a_k is the discrete cross-sectional area of the kth member, which is chosen from steel pipes in an available profile list $(\tilde{\mathbf{A}})$, and b_j is the cost of the jth node; each truss design must perform design constraints on natural frequency (g_f), stresses/buckling (g_σ), and displacements (g_δ) [59]. *NMG* is the number of member groups (i.e. number of design variables). Also, *NM* and *nj* are the number of members and nodes, respectively, in the truss structure.

This is a well-known example that has been studied by many researchers. According to the results presented so far in different papers, different numbers have been used for node weight (kg), modulus of elasticity (E), and material density (ρ). In this paper, three different designs, including changes in these parameters were considered, as shown in Table (1).

Table 1: Different cases analyzed for the 10 bar plane truss

Case	E(Gpa)	ρ(kg/m^3)	m (kg)	Authors
1	68.95	2767.99	453.60	Miguel et al. **[57]**
2	68.90	2770.00	454.00	Kaveh and Javadi [58]
3	69.80	2770.00	454.00	Kaveh and Javadi [58]

According to Table (2), the weight of the truss, the mean and standard deviation of the WOA algorithm results are compared with the previous works. It can be seen that the WOA algorithm has a high power, such that it finds a better solution in all cases. Also, for all design scenarios, the number of truss analyses needed to achieve the optimal weight is lower in the WOA algorithm, as compared to that of the previous works.

Table 2: Best designs and statistical results for the three cases of the 10 bar plane truss

Member	Areas (cm^2)								
	Case1			***Case2***			***Case3***		
	Miguel et al. **[57]**	M.S. Gonçalves et al. [56]	WOA	Kaveh and Javadi [58]	M.S. Gonçalves et al. [56]	WOA	Kaveh and Javadi [58]	M.S. Gonçalves et al. [56]	WOA
1	36.198	35.996	**35.4918**	35.540	35.398	**35.333**	34.793	34.282	**35.3315**
2	14.030	15.045	**14.6741**	15.293	15.112	**14.960**	15.245	15.062	**14.7246**
3	34.754	35.218	**35.6088**	35.784	36.174	**35.921**	35.562	36.205	**34.9724**
4	14.900	15.404	**14.7212**	14.606	14.762	**14.907**	13.836	14.566	**14.9486**
5	0.654	0.645	**0.6491**	0.646	0.645	**0.645**	0.646	0.645	**0.6451**
6	4.672	4.599	**4.6370**	4.626	4.620	**4.627**	4.583	4.554	**4.5502**
7	23.467	23.498	**24.1684**	24.779	24.433	**24.038**	25.535	24.120	**23.3924**
8	25.508	24.004	**24.2446**	23.310	23.723	**24.069**	22.300	23.172	**23.8201**
9	12.707	12.372	**12.5436**	12.482	12.334	**12.852**	11.614	12.080	**12.4722**
10	12.351	12.872	**12.5258**	12.675	12.602	**12.358**	13.072	12.641	**12.3776**
Mass (kg)	531.280	530.98	**530.76**	532.11	532.11	**532.1040**	524.88	524.70	**524.52**
Mean	535.07	531.39	**530.83**	-	532.72	**532.29**	-	525.68	**524.80**
Standard deviation	3.64	0.52	**0.036**	2.37	0.76	**0.112**	2.25	0.64	**0.4379**
NFE	50000	50000	**24435**	21000	21000	**20638**	21000	21000	**20193**

*NFE represents the number of structural analyses by which the algorithm first achieves the minimum weight.

6.1 Introducing steel frame models and controlling structural design criteria

In this paper, three two-dimensional 8, 16 and 24-story frames were modeled to compare different design methods. The number of frame openings, the length of each opening and the height of the stories were 5, 5 and 3 meters, respectively. The dead and live loads on the stories were 5000 and 2000 kg / m, respectively. All sections used in the modeling are selected from W-shaped sections of the AISC database [48]. The important point that has been observed in the selection of sections was that all selected sections had seismic compression conditions. The specifications of the steel materials modeled in this paper are as described in Table (3).

Table 3: Specifications of steel materials

W=7850 $\frac{kg}{m^3}$	Unit weight of the material volume
E=2.0e+10 $\frac{kgf}{m^2}$	Modulus of elasticity
ν=0.3	Poisson's ratio
F_y=24e+6 $\frac{kgf}{m^2}$	Stress yield of steel materials
F_u=37e+6 $\frac{kgf}{m^2}$	Ultimate tensile stress of steel materials

Seismic loading in the static analysis of structures was performed according to ASCE7-16 [59]. For designing by the LRFD method, the design location of the frames in an area with the soil class D (an area with a very high relative risk) was assumed in accordance with the above codes; the use of the building was a residential one. According to ASCE 7-16 standards [59], the coefficient $S_1 = 0.63$ and the coefficient $S_S = 1.5$ were considered. Permissible relative displacement control was performed based on 0.02. The modeling and design of the frame were done using the LRFD method, by the SAP2000 software [61].

In these frames, the lateral load-resistant system is a special steel moment frame. All nodes of the structure are rigid.

The codes related to the WOA optimization algorithm and the relation between modeling and designing frames by Energy method have been performed in the Matlab software [49]; nonlinear static analysis of frames has been performed in the SAP2000 software [61]. In this article, SAP2000 software [61] was linked to the Matlab software [49] to optimize the frames. It should be noted that, for all examples, the population number in the WOA algorithm was 50 and the number of iterations was assumed to be 200. The types of sections are shown in Fig. 10 and the section specifications of the three methods are shown in Tables 3 to 6.

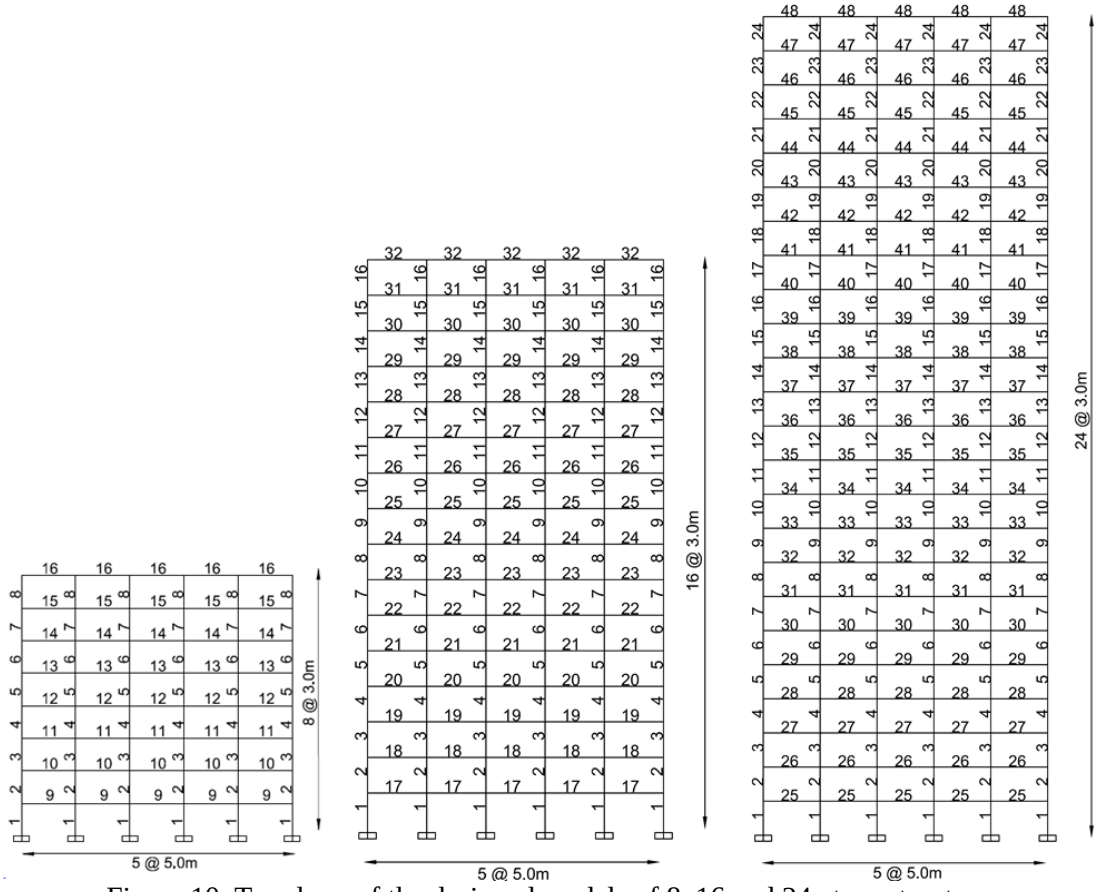

Figure 10. Typology of the designed models of 8, 16 and 24-story structures

The results related to the Energy method in shifting the target locations IO, LS and CP were obtained. The results of shifting the target location of LS, according to Table (3-5), are presented as the design results of this method. Also, by performing the optimization through the E-WOA method, the final result is presented for all three examples according to Tables (4-6) for the E-WOA method.

Table 4: Final design results of Energy method and E-WOA methods in 8-story structures

Type number and cross section assigned to each of the beams and columns of the frame													Design methods
13	**12**	**11**	**10**	**9**	**8**	**7**	**6**	**5**	**4**	**3**	**2**	**1**	
W21x50	W21x55	W21x55	W24x55	W24x55	W21x55	W24x76	W30x90	W27x84	W30x90	W30x108	W33x118	W33x130	Energy method
W21x50	W21x55	W24x55	W24x55	W21x62	W18x35	W24x55	W24x76	W24x84	W30x99	W30x116	W36x135	W40x149	E-WOA
										16	**15**	**14**	
										W14x34	W18x40	W21x44	
										W16x26	W18x35	W21x44	

Table 5: Final design results of Energy method and E-WOA methods in 16-story structures

Type number and cross section assigned to each of the beams and columns of the frame													Design methods
13	**12**	**11**	**10**	**9**	**8**	**7**	**6**	**5**	**4**	**3**	**2**	**1**	

W33 x130	W40 x149	W40 x167	W40 x189	W40 x199	W40 x215	W44 x230	W44 x230	W44 x262	W44 x262	W44 x262	W44 x290	W44 x290	Energy method
W27 x146	W27 x161	W30 x173	W30 x191	W30 X191	W33 X201	W33 X201	W33 X201	W33 X201	W33 X221	W36 X230	W40 X249	W44 x262	E-WOA
26	**25**	**24**	**23**	**22**	**21**	**20**	**19**	**18**	**17**	**16**	**15**	**14**	
W21 x50	W21 x50	W21 x55	W21 x55	W21 x55	W21 x55	W21 x55	W21 x5	W21 x55	W21 x55	W21 x50	W27 x84	W30 x108	
W21 x55	W24 x55	W24 x55	W21 x62	W21 x62	W21 x62	W21 x62	W21 x62	W21 x62	W21 x62	W18 x50	W24 x84	W27 x114	
							32	**31**	**30**	**29**	**28**	**27**	
							W16 x31	W18 x35	W18 x40	W21 x44	W21 x44	W18 x50	
							W16 x31	W18 x40	W21 x44	W21 x50	W21 x55	W21 x55	

Table 6: Final design results of Energy method and E-WOA methods in 24-story structures

Type number and cross section assigned to each of the beams and columns of the frame													**Design methods**
13	**12**	**11**	**10**	**9**	**8**	**7**	**6**	**5**	**4**	**3**	**2**	**1**	
W40 x372	W40 x397	W40 x431	W40 x503	W40 x503	W40 x503	W40 x503	W40 x593	W40 x593	W40 x593	W40 x593	W40 x593	W36 x650	Energy method
W27 x539	W30 x357	W30 x357	W30 x357	W30 x357	W33 x318	W33 x318	W33 x318	W33 x354	W33 x354	W33 x354	W36 x359	W40 x362	E-WOA
26	**25**	**24**	**23**	**22**	**21**	**20**	**19**	**18**	**17**	**16**	**15**	**14**	
W21 x68	W21 x68	W21 x55	W30 x90	W33 x130	W40 x149	W40 x183	W40 x211	W44 x230	W44 x262	W44 x290	W40 x324	W44 x335	
W24 x76	W24 x76	W24 x68	W27 x129	W27 x178	W27 x235	W27 x281	W27 x307	W27 x368	W27 x368	W27 x368	W27 x539	W27 x539	
39	**38**	**37**	**36**	**35**	**34**	**33**	**32**	**31**	**30**	**29**	**28**	**27**	
W21 x62	W21 x62	W24 x62	W24 x62	W24 x62	W24 x62	W21 x68	W21 x68	W21 x68	W21 x68	W21 x68	W21 x68	W21 x68	
W24 x68	W24 x76	W24 x76	W24 x76	W24 x76	W24 x76	W24 x76	W24 x76	W24 x76	W24 x76	W24 x76	W24 x76	W24 x76	
				48	**47**	**46**	**45**	**44**	**43**	**42**	**41**	**40**	
				W16 x31	W16 x40	W21 x44	W18 x50	W21 x50	W21 x55	W21 x55	W24 x55	W24 x55	
				W16 x40	W21 x44	W21 x55	W24 x55	W21 x62	W24 x62	W21 x68	W24 x68	W24 x68	

6.2 Controlling the results of frame analysis

After designing the structure in accordance with the AISC 2016 standard [48] and performing all controls required by the codes, the results of stories drift, the ratio of minimum, the maximum average stress of members and the ratio of beam capacity to columns are shown in Tables 7 to 9.

Table 7: Results of the analysis of Energy method and E-WOA methods in 8-story structures

Average capacity of beams to columns	Minimum capacity of beams to columns	Maximum capacity of beams to columns	Average stress ratio	Minimum stress ratio	Maximum stress ratio		Design methods
0.9492	0.3757	1. 0	0.7655	0.5634	0.9722	**beams**	Energy method
			0.6882	0.3155	1.032	**columns**	
0.8305	0.01	1.0	0.7655	0.5634	0.9722	**beams**	**E-WOA**
			0.6882	0.3155	1.032	**columns**	

Table 8: Results of the analysis of Energy method and E-WOA methods in 16-story structures

Average capacity of beams to columns	Minimum capacity of beams to columns	Maximum capacity of beams to columns	Average stress ratio	Minimum stress ratio	Maximum stress ratio		Design methods
0.310	0.01	0.7412	0.8532	0.5126	1.10	**beams**	Energy method
			0.5619	0.2845	0.8175	**columns**	
0.3348	0.01	0.8692	0.8306	0.5055	1.0659	**beams**	**E-WOA**
			0.5623	0.2948	0.7751	**columns**	

Table 9: Results of the analysis of Energy method and E-WOA methods in 24-story structures

Average capacity of beams to columns	Minimum capacity of beams to columns	Maximum capacity of beams to columns	Average stress ratio	Minimum stress ratio	Maximum stress ratio		Design methods
0.1937	0.01	0.6812	0.8429	0.4691	1.00	**beams**	Energy method
			0.4333	0.2395	0.6505	**columns**	
0.2492	0.01	0.8702	0.8083	0.3951	1.09	**beams**	**E-WOA**
			0.4885	0.3425	0.7284	**columns**	

One of the most important controls performed on a special moment frame or a highly ductile moment frame is the strong column-weak beam control. This rule causes the plastic hinge to be formed first in the beams, so that the structure can withstand further deformation without any reduction of strength. As can be seen from the above tables, the capacity of the beams to the columns in the E-WOA is, on average, lower than that in the Energy methods.

6.2.1 Lateral displacement control of the structure

Lateral displacement control of the structure is performed according to the clause 12.12.1 of the ASCE7-16 code [59]. According to this, the relative nonlinear lateral displacement of the story δ_M will be calculated by Equation 33. In this relation, C_d is the magnification coefficient of the lateral displacement of the structure due to the nonlinear behavior and δ_{xe} is the relative linear displacement of the story. Also, I_e is the coefficient of the importance of the building.

$$\delta_M = \frac{C_d \times \delta_{xe}}{I_e} \tag{33}$$

The value of δ_M, which is obtained by considering the effects of P-Δ, should not exceed the allowable value of Equation 34. In the above relation, h_{sx} is the story height.

$$\Delta_a = 0.02\, h_{sx} \tag{34}$$

Fig. 11 shows the relative lateral displacement diagrams of 8, 16 and 24-story structures in Energy and E-WOA methods.

Fig. 12 shows the results of the structural drift in the target displacement defined for the CP level. It can be seen that the drift of both energy methods and EWOA did not exceed the permissible value defined in the ASCE41-17 code [47].

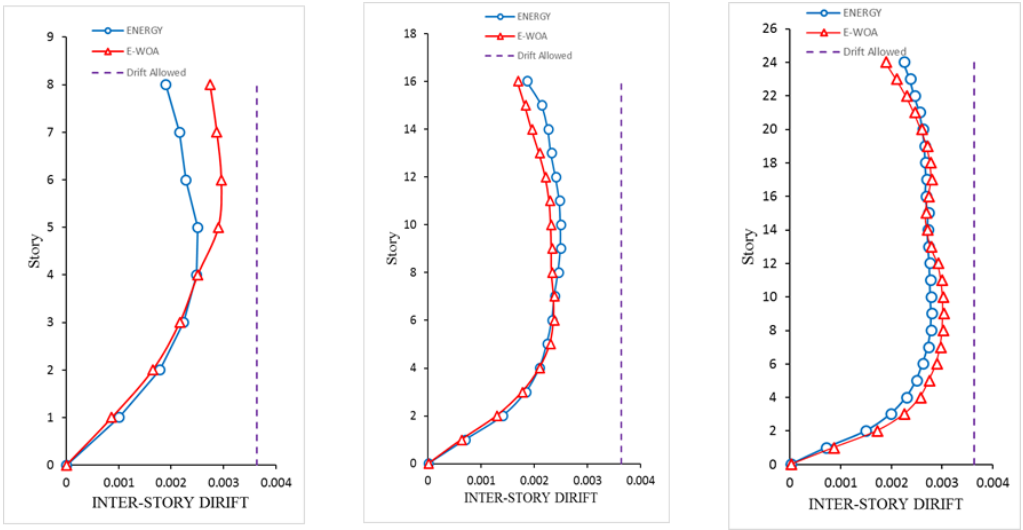

Figure 11. Comparison diagram of the relative lateral displacement of the buildings 8, 16 and 24

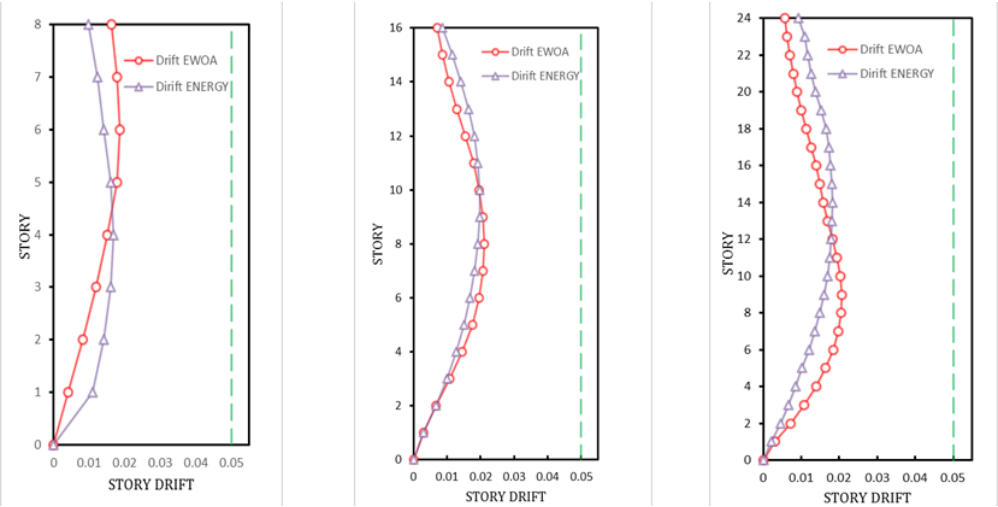

Figure 12. Comparison diagram of the relative lateral displacement of the buildings 8, 16 and 24 at target displacement levels

7. RESULTS OF THE NONLINEAR STATIC ANALYSIS OF FRAMES

In all three examples, following the design of the structures by Energy and E-WOA methods, for the purpose of comparison, after adjusting the plastic hinges of the members and nonlinear static analysis, as well as applying dead and live loads as the dynamic loads, by continuing to apply gravity loads, pushing of structures is done with the lateral static load pattern.

7.1 Example 1: 8-story frame

Fig. 13 shows the plastic hinges created on 8-story frames designed with Energy and E-WOA methods.

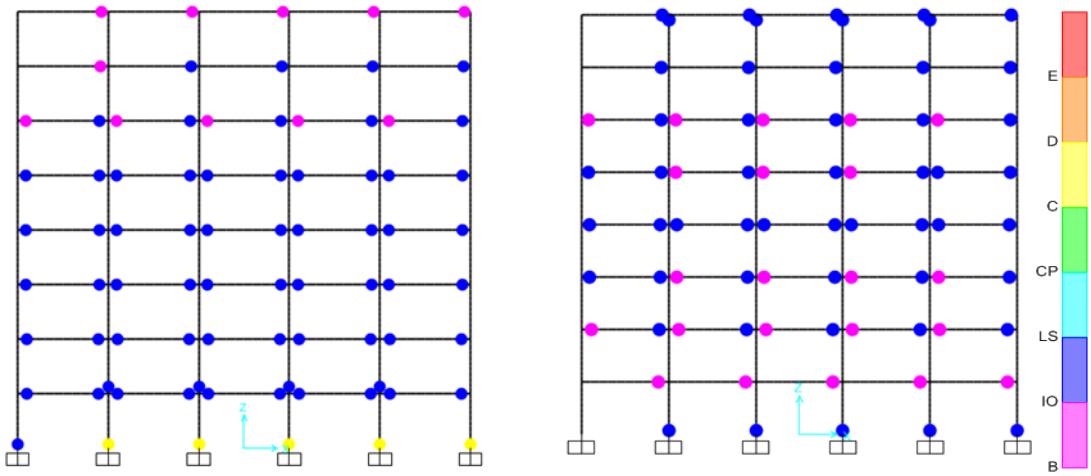

Energy Method E-WOA

Figur 13. Plastic hinge created on an 8-story frame designed by three methods: Energy and E-WOA

Figs. 14 and 15 have been used to better understand the process of forming plastic hinges on the frames. In these figures, on the diagram, the pushing images of plastic hinge formation in different stages are shown.

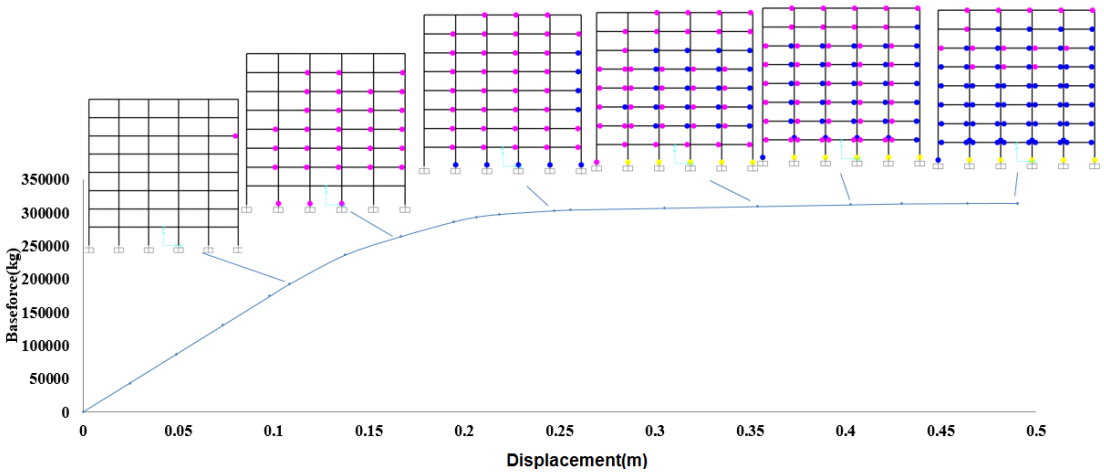

Figure 14. Push-over graph of an 8-story frame designed by the Energy method

In the graph of Fig. 14, which is related to the Energy design method, the nonlinear capacity of the members is used appropriately.

Fig. 14 shows the order of hinges formation in the members. In this method, after obtaining the moment of the beam design, the beam design is done and the columns are designed as a capacity. The problem in these steps is that due to the limited number of sections in the design, we have to use sections with a higher capacity than the value obtained. So, in this method, we do not reach exactly the defined goals and the appropriate

pattern considered for the formation of hinges could not be realized. One of the goals of combining the energy method with the WOA algorithm is to solve this problem, which is almost realized in the EWOA method. Further, a more favorable weight could be obtained for the structure.

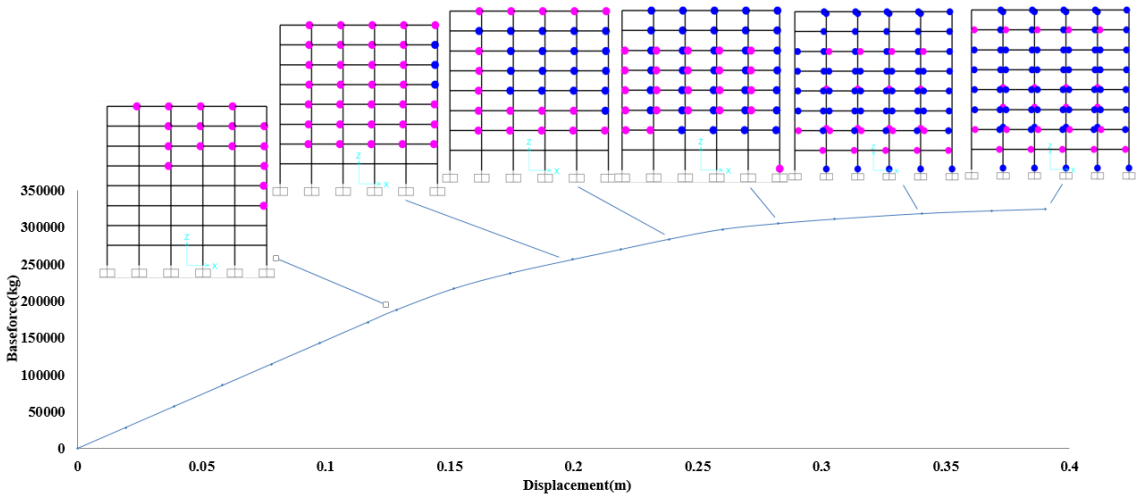

Figure 15. Push-over graph of an 8-story frame designed by the E-WOA method

Fig. 15 shows the results of the optimization method introduced in this paper as E-WOA. This method could improve the nonlinear performance of the structure by maintaining the optimality criteria defined for the structure.

In the E-WOA method, the result is obtained after about 9308 structural analyses. The method convergence history plot is shown in Fig. 16. It should be noted that despite the lower weight obtained for the E-WOA method, the Energy method could achieve good results in the first step and the modifications of the Energy method have been done correctly.

In Fig. 17, the push-over graphs of the Energy and E-WOA design methods, along with the weight of the structure, are compared. The weight of the structure by Energy method is 34.634 tons. After combining this method with the WOA optimization algorithm, while maintaining the appropriate nonlinear behavior of the structure, the weight of the structure by E-WOA method was 34.380 tons, which was less than that by the Energy method.

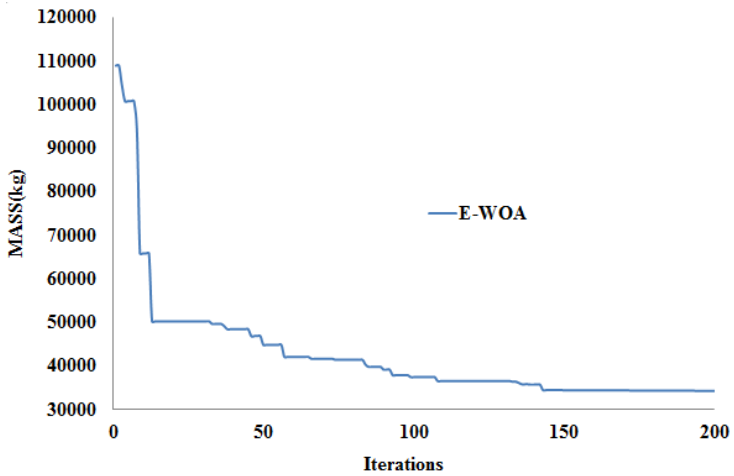

Figure 16. The Convergence History plot of the E-WOA Method (8-story)

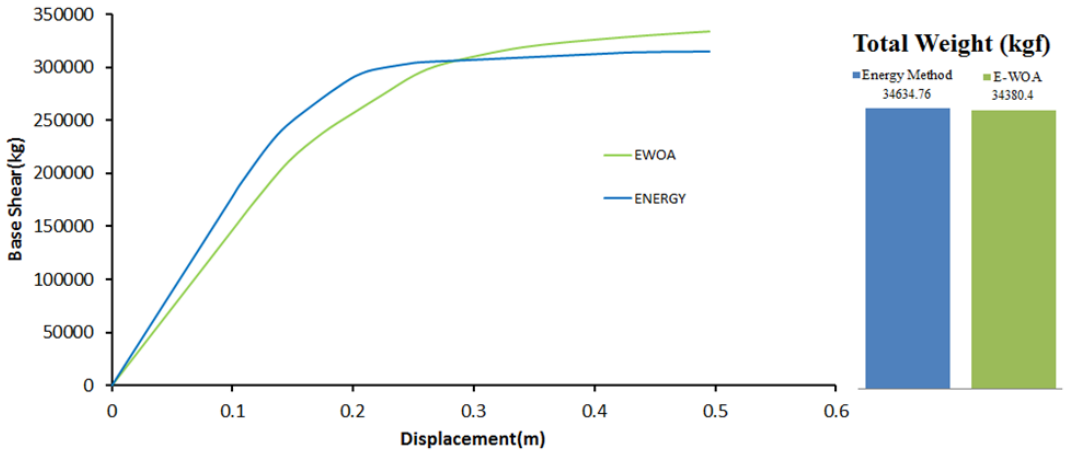

Figure 17. Comparison of the push diagrams and the weight of the 8-story steel frame designed with three methods including Energy and E-WOA

7.2 Second example: 16-story frame

Fig. 18 shows the plastic hinges created on 16-story frames designed by three methods: Energy methods and E-WOA.

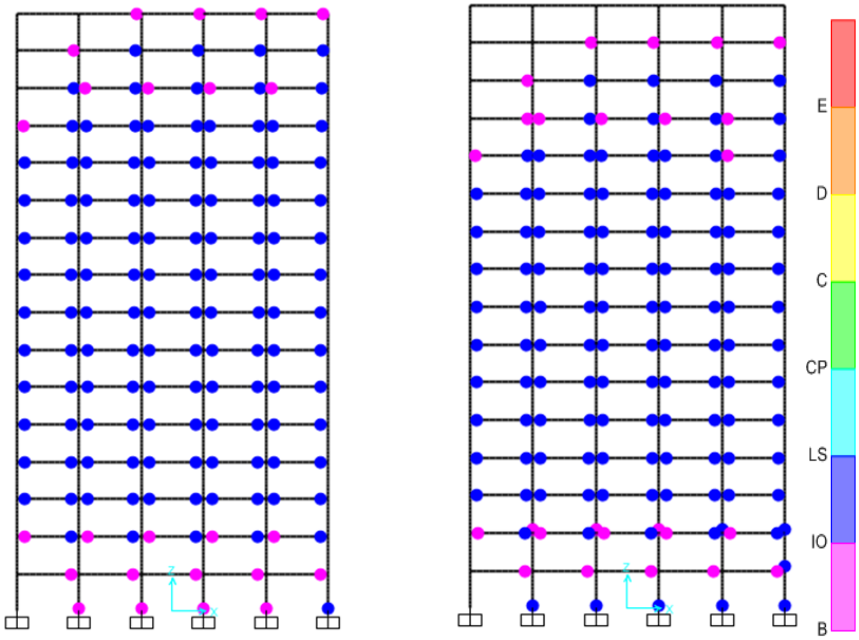

Energy Method E-WOA

Figure 18. Plastic created on 16-story frames designed with three methods including Energy and E-WOA

Figs. 19 and 20 have been used to better understand the process of forming plastic hinges on frames. In these figures, on the push diagram, the images of plastic hinge formation in different stages are shown.

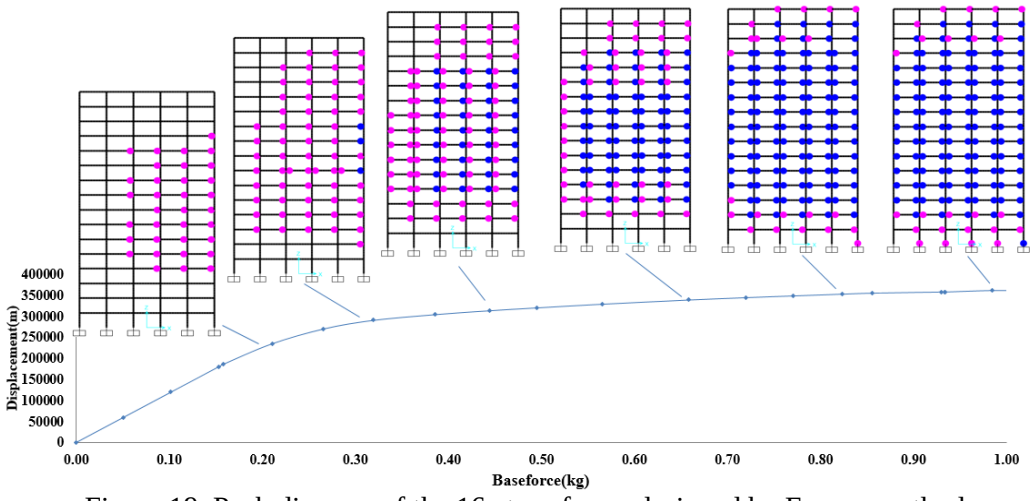

Figure 19. Push diagram of the 16-story frame designed by Energy method

Fig. 19 shows the push diagram along with the steps of plastic hinge created at the members on the frame designed by the Energy method.

In this figure, the distribution of hinges in different steps to the target displacement is shown; as can be seen, the Energy method has achieved good results; to improve these results in the combined method, we see a reduction in structure weight. Meanwhile, in terms of nonlinear static analysis, the push diagram of structure is also improved in the EWOA method, as compared to the Energy method.

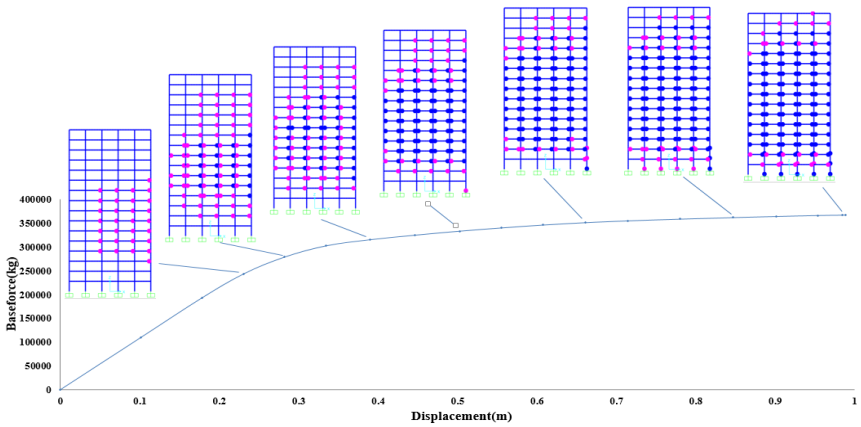

Figure 20. Push diagram of the 16-story frame designed by the E-WOA method

Fig. 20 shows the results of the optimization method introduced in this paper as E-WOA. This method obtained good results in the nonlinear static analysis; so, by maintaining the optimality criteria defined for the structure, it can improve the nonlinear performance of the structure.

In E-WOA method, the results could be obtained after about 9583 structural analyses. The convergence history plot of the method is shown in Fig. 21. In this example, according to Fig. 22, the weight obtained from the E-WOA method is equal to 109.898 tons; this, compared to the Energy method with a weight of 112.815 tons, is a suitable weight reduction. Fig. 21 compares the push diagrams of three different methods for designing structures. It can be seen that the nonlinear performance of the structure is better in the E-WOA design mode than in the Energy method.

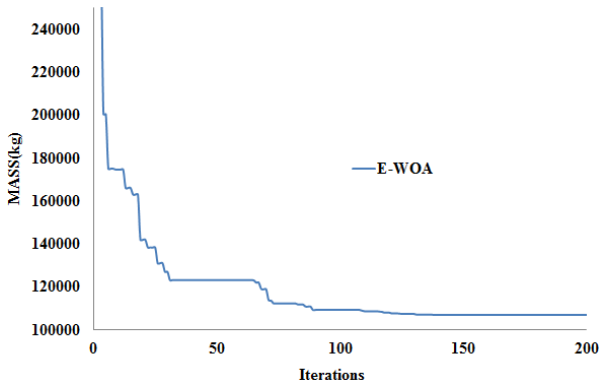

Figure 21. Convergence History plot of the E-WOA Method (16-Story)

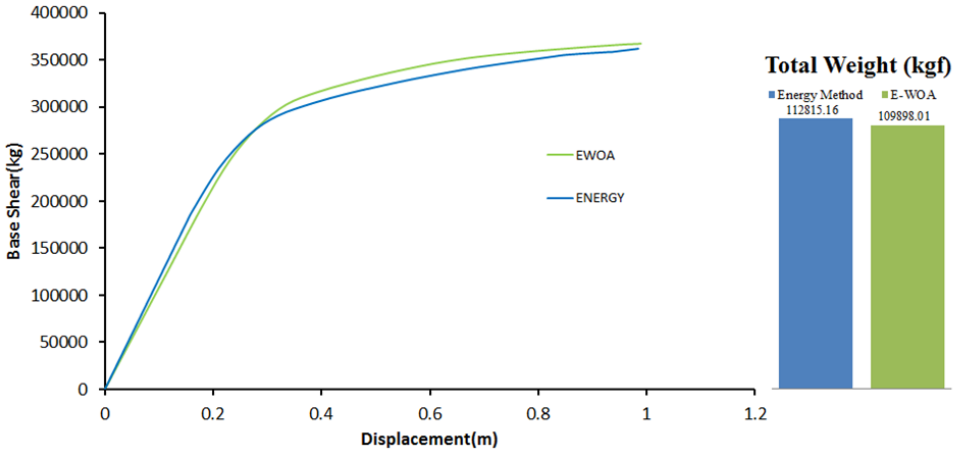

Figure 22. Comparison of the push diagram and weight of 16-story steel frame designed with three methods including Energy and E-WOA

7.3 Third example: 24-story frame

Fig. 23 shows the plastic hinge created on 24-story frames designed by three methods: Energy and E-WOA.

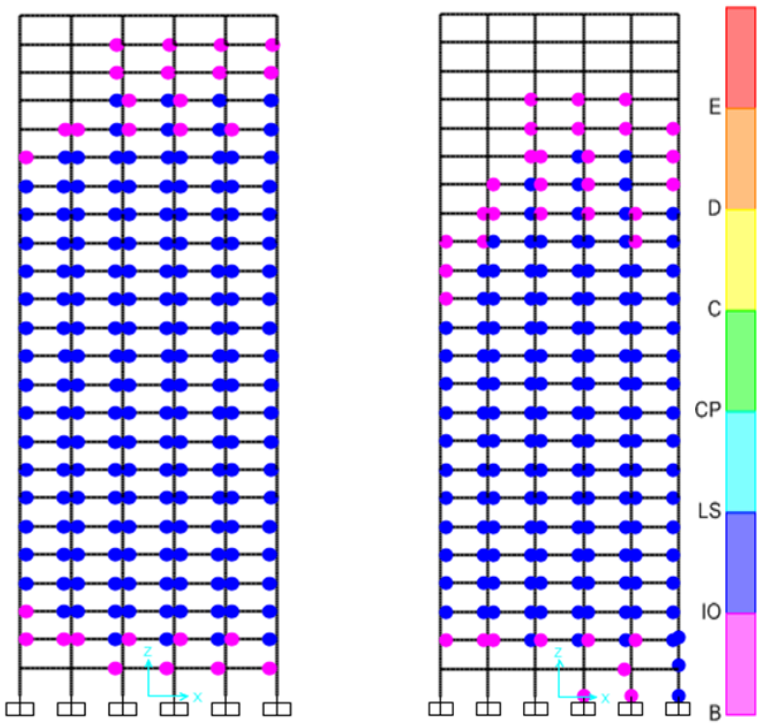

Energy Method E-WOA

Figure 23. Plastic hinge created on 24-story frames designed with three methods: Energy and E-WOA

The process of forming plastic hinges on the frames is according to Figs. 24 and 25.

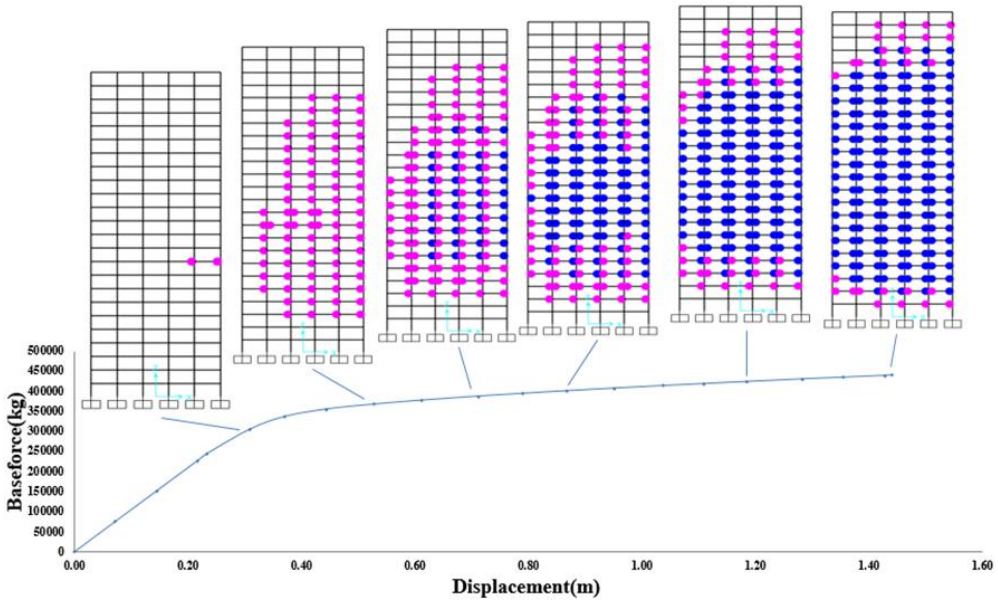

Figure 24. Push diagram of a 24-story frame designed by the Energy method

Fig. 24 shows the push diagram along with the steps of forming plastic hinges of the members on the frame designed by Energy method. In this figure, as can be seen, the Energy design method uses the nonlinear capacity of the members more appropriately.

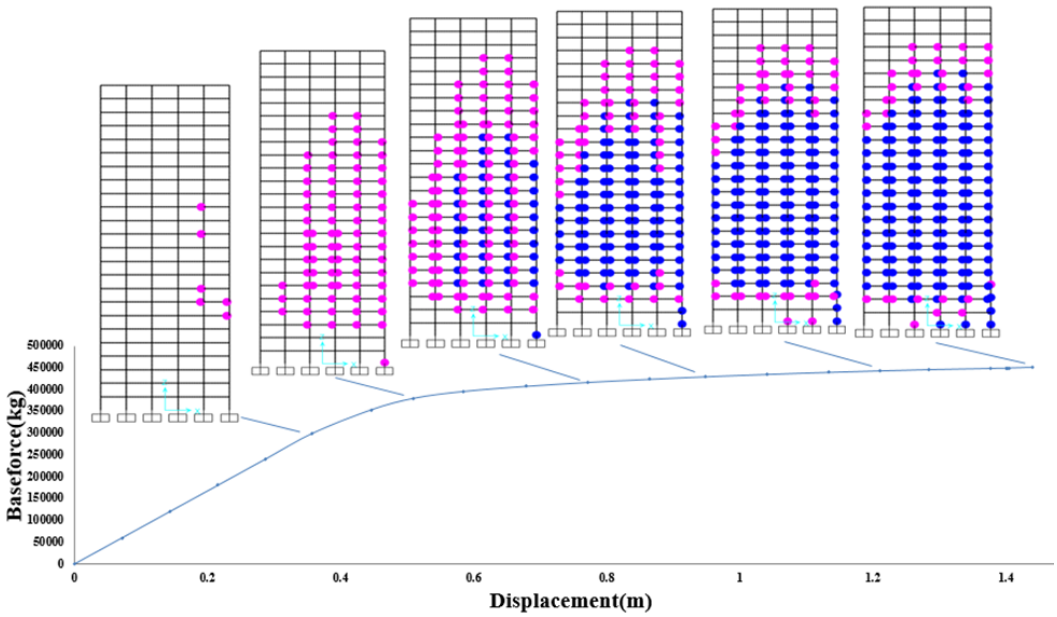

Figure 25. Push diagram of the 24-story frame designed by the E-WOA method

Fig. 25 shows the results of the E-WOA method. This method led to obtaining good results in static nonlinear analysis; by maintaining the optimality criteria defined for the structure, it can improve the nonlinear performance of the structure. In the E-WOA method, the results are obtained after about 9978 structural analyses. The convergence history plot of the method is shown in Fig. 26. In this example, according to Fig. 27, the weight obtained from the E-WOA method is equal to 277.795 tons; this, compared to the Energy method with a weight of 296.413 tons, is a suitable weight reduction.

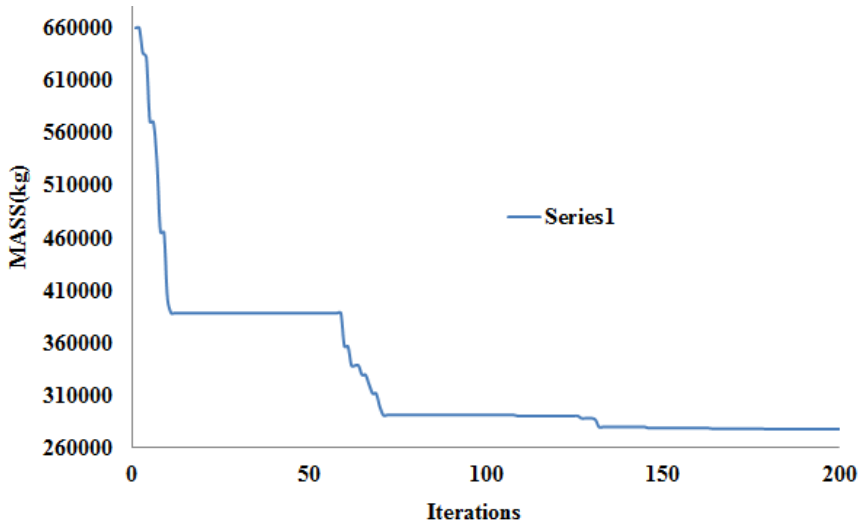

Figure 26. The Convergence History plot of the E-WOA Method (24-Story)

In Fig. 27, the push diagram of the two structural design modes is also compared with each other. It can be seen that the nonlinear performance of the structure is more suitable in the E-WOA design mode than in the Energy method.

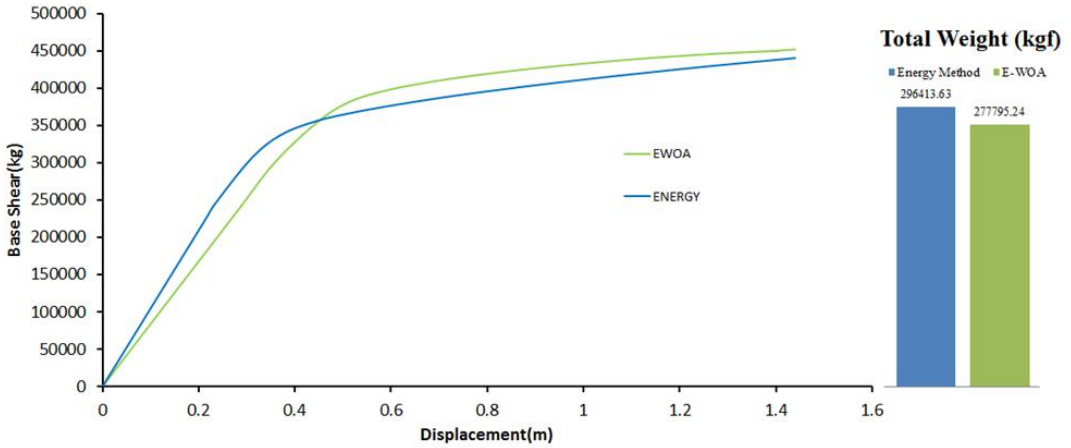

Figure 27. Comparison of the push diagram and weight of the 24-story steel frame designed with three methods including Energy and E-WOA

In general, according to the results of the previous three examples, it can be said that the Energy method has a good performance for the frames; it could be even improved by modifying it through the WOA algorithm. In the 8-story frame, the weight of the structure is almost equal in the two methods; the more the height of the structure and the number of floors, the higher the difference in the weight obtained from the Energy method and EWOA, thus indicating the desirable combination of the two methods. It also shows that EWOA, while increasing the nonlinear performance of the structure, as compared to the Energy method, also reduces the weight of the structure.

8. CONCLUSION

In this paper, based on the balance of the input and output energy of the structure due to lateral and gravity loads, by applying modifications in this method, the design of moment frames with different numbers of stories was done. One of the modifications made for this method was the use of the effects of different building modes in estimating the input energy of the earthquake; the other modification was the use of the effect of internal damping of materials in calculating the energy absorbed by the frame members. The Whale Algorithm (WOA), also known as E-WOA, has been used to improve and optimize energy design results. The objective function of the two-stage E-WOA algorithm is in the first stage to achieve the desired balance between the input and output energy of the structure; then in the second stage, it is the weight of the frame and the proper formation of plastic hinges. Problem constraints are the performance level criteria of ASCE41-17, stress and uniformity of the drift distribution at the frame height. In this paper, to compare the results obtained for E-WOA methods, the frames were designed using the Energy method. The criteria for comparing the results included the structure weight, the way hinges were distributed in the height of the structure, the analysis of the structure's push diagram, and the way the capacities of linear and nonlinear areas were used. Three 8, 16 and 24-story frames were considered as the examples. The results showed that by increasing the frame height, the weight of the frame by E-WOA method was less than that by Energy method in all three examples. Distribution of plastic hinges in stories, including beams and columns, was more desirable in E-WOA than in the Energy method. Overall, with the modifications made to the input-output energy balance relations to the structure, with a reliable approximation, the use of the energy method led to obtaining more favorable results; so, the improved behavior of the structure was evident. Also, compared to the combination of this method with WOA algorithm, it could achieve a suitable design with an optimal nonlinear performance in just one step and with much less computational volume.

REFERENCES

1. Housner GW. Limit design of structures to resist earthquakes, in *Proceedings of the 1st World Conference on Earthquake Engineering* 1956; pp. 5.1-5.13.
2. Manfredi G. Evaluation of seismic energy demand, *Earthq Eng Struct Dyn* 2001; **30**(4):

485–499.
3. Sucuoglu H, Erberik A. Energy-based hysteresis and damage models for deteriorating systems, *Earthq Eng Struct Dyn* 2004; **33**(1): 69-88.
4. Massumi A, Monavari B. Energy based procedure to obtain target displacement of reinforced concrete structures, *Struct Eng Mech* 2013; **48**(5): 681-95.
5. Paolacci F. An energy-based design for seismic resistant structures with viscoelastic dampers, *Earthq Struct* 2013; **49**(2): 219-39.
6. Choi H, Kim J. Evaluation of seismic energy demand and its application on design of buckling-restrained braced frames, *Struct Eng Mech* 2009; **31**(1): 93–112.
7. Dindar AA, Yalçin C, Yüksel E, Özkaynak H, Büyüköztürk O. Development of earthquake energy demand spectra, *Earthq Spectra* 2015; **31**(3): 1667-89.
8. Wang, F, Zhang N, and Huang, Z (2016) Estimation of earthquake induced story hysteretic energy of multi-Story buildings, Earthq. Struct., 11(1), pp. 165-178.
9. Dogru S, Aksar B, Akbas B, Shen J. Parametric study on energy demands for special steel concentrically braced frames, *Steel Compos Struct* 2017; **24**(2): 265-76.
10. Mezgebo MG, Lui EM. A new methodology for energy-based seismic design of steel moment frames, *Earthq Eng Eng Vib* 2017; **16**(1): 131-62.
11. Ozsarac V, Karimzadeh S, Erberik MA, Askan A. Energy-based response of simple structural systems by using simulated ground motions, *Procedia Eng* 2017; **199**: 236-41.
12. Ucar T, Merter O. Derivation of energy-based base shear force coefficient considering hysteretic behavior and Pdelta effects, *Earthq Eng Eng Vib* 2018; **17**(1): 149-63.
13. Merter O. An investigation on the maximum earthquake input energy for elastic SDOF systems, *Earthq Struct* 2019; **16**(4): 487-99.
14. Santarsiero M, Bedon C, Moupagitsoglou K. Energy-based considerations for the seismic design of ductile and dissipative glass frames, *Soil Dyn Earthq Eng* 2019: **125**: 105710.
15. Ucar T. Computing input energy response of MDOF systems to actual ground motions based on modal contributions, *Earthq Struct* 2020; **18**(2): 263-73.
16. Zhou Y, Song G, Huang S, Wu H. Input energy spectra for self-centering SDOF systems, Soil Dyn Earthq Eng 2019; **121**: 293-305.
17. Qiu C, Qi J, Chen C. Energy-based seismic design methodology of SMABFs using hysteretic energy spectrum, *J Struct Eng* 2020; **146**(2): 4019207.
18. SEAOC V, others. Performance based seismic engineering of buildings, Structural Engineers Association of California, Sacramento, Calif, 1995.
19. FEMA-356. Prestandard and commentary for the seismic rehabilitation of buildings .Federal Emergency Management Agency, Washington, DC, 2000
20. FEMA. FEMA 695 - Quantification of building seismic performance factors, Federal Emergency Management Agency, Washington, DC, 2009.
21. Holland JH. Adaptation in natural and artificial systems, University of Michigan Press, 1975
22. Geem ZW, Kim JH, Loganathan GV. A new heuristic optimization algorithm: harmony search, Simulation 2001; **76**(2): 60-8.
23. Dorigo M. Optimization, Learning and Natural Algorithms, Ph.D. Thesis, Politecnico di Milano, Milan, Italy.

24. Karaboga D. An Idea Based on Honey Bee Swarm for Numerical Optimization, Technical Report TR06, Erciyes University, 2005.
25. Eberhart R, Kennedy J. A new optimizer using particle swarm theory, *in MHS'95 Proceedings of the Sixth International Symposium on Micro Machine and Human Science* 1995, pp. 39-43.
26. Atashpaz-Gargari E, Lucas C. Imperialist competitive algorithm: An algorithm for optimization inspired by imperialistic competition, *in 2007 IEEE Congress on Evolutionary Computation* 2007; pp. 4661-7.
27. Kaveh A, Talatahari S. Imperialist competitive algorithm for engineering design problems, *Asian J Civil Eng* 2010; **11**(6): 675-97.
28. Yang XS. Firefly algorithms for multimodal optimization, *Int Symp Stoch Algorithms* 2009; 169-78.
29. Yang XS. *A New Metaheuristic Bat-Inspired Algorithm, in Nature Inspired Cooperative Strategies for Optimization (NICSO 2010)*, Springer, pp. 65-74.
30. Kaveh A, Farhoudi N. A new optimization method: Dolphin echolocation, *Adv Eng Softw* 2013; **59**: 53-70.
31. Mashayekhi M, Salajegheh E, Dehghani M. A new hybrid algorithm for topology optimization of double layer grids, *Int J Optim Civil Eng* 2015; **5**(3): 353-74.
32. Mashayekhi M, Salajegheh J, Fadaee MJ, Salajegheh E. A two-stage SIMP-ACO method for reliability-based topology optimization of double layer grids, *Int J Optim Civil Eng* 2011; **1**(4): 521-42.
33. Fragiadakis M, Lagaros ND, Papadrakakis M. Performance-based multiobjective optimum design of steel structures considering life-cycle cost, *Struct Multidiscip Optim* 2006; **32**(1): 1-11.
34. Talatahari S. Optimum performance-based seismic design of frames using metaheuristic optimization algorithms, *Metaheuristic Appl Struct Infrastructures* 2013; 419-37.
35. Kaveh A, Nasrollahi A. Performance-based seismic design of steel frames utilizing charged system search optimization, *Appl Soft Comput* 2014; **22**: 213-21.
36. Gholizadeh S, Poorhoseini H. Optimum design of steel frame structures by a modified dolphin echolocation algorithm, *Struct Eng Mech* 2015; **55**(3): 535-54.
37. Karimi F, Vaez SRH. Two-stage optimal seismic design of steel moment frames using the LRFD-PBD method, *J Constr Steel Res* 2019; **155**: 77-89.
38. Gholizadeh S, Danesh M, Gheyratmand C. A new Newton metaheuristic algorithm for discrete performance-based design optimization of steel moment frames, *Comput Struct* 2020; **234**: 106250.
39. Degertekin SO, Tutar H, Lamberti L. School-based optimization for performance-based optimum seismic design of steel frames, *Eng Comput* 2021; **37**(4): 3283-97.
40. Hasan R, Xu L, Grierson DE. Push-over analysis for performance-based seismic design, *Comput Struct* 2002; **80**(31): 2483-93.
41. Grierson DE, Gong Y, Xu LEI. Optimal performance-based seismic design using modal pushover analysis, *J Earthq Eng* 2006; **10**(1): 73-96.
42. Salajegheh E, Mohammadi A, Ghaderi Sohi S. Optimum performance based design of concentric steel braced frames, *in the 14 th World Conference on Earthquake Engineering*, 2008.

43. Kaveh A, Azar BF, Hadidi A, Sorochi FR, Talatahari S. Performance-based seismic design of steel frames using ant colony optimization, J Constr Steel Res 2010; **66**(4): 566-74.
44. Tehranizadeh M, Moshref A. Performance-based optimization of steel moment resisting frames, *Sci Iran* 2011; **18**(2): 198-204.
45. Gholizadeh S, Kamyab R, Dadashi H. Performance-based design optimization of steel moment frames, *Int Optim Civil Eng* 2013, **3**(2): 327-43.
46. Gholizadeh S. Performance-based optimum seismic design of steel structures by a modified firefly algorithm and a new neural network, *Adv Eng Softw* 2015; **81**: 50–65.
47. ASCE 41-17. Seismic evaluation and retrofit of existing buildings, American Society of Civil Engineers, 2017.
48. Committee A, others, Seismic Provision for Structural Steel Buildings (ANSI/AISC 341-16). Chicago: American Institute of Steel Construction, 2016.
49. Mathworks I. MATLAB and statistics toolbox release 2012b, Natick (Massachusetts, United States), 2012.
50. Banihashemi MR, Mirzagoltabar A, Tavakoli H. Development seismic design of steel moment frames and the evaluation by energy spectrum method, *Indian J Sci Technol* 2014, **7**(10): 1699-1711.
51. Bai J, Ou J. Plastic limit-state design of frame structures based on the strong-column weak-beam failure mechanism, *in Proceedings of the 15th World Conference on Earthquake Engineering*, 2012.
52. Leelataviwat S, Goel SC, Stojadinović B. Toward performance-based seismic design of structures, *Earthq Spectra* 1999, **15**(3): 435-61.
53. Akiyama H. Earthquake-Resistant Limit-State Design for Buildings, University of Tokyo Press, Tokyo, Japan, 1985.
54. Mirjalili S, Lewis A. The whale optimization algorithm, *Adv Eng Softw* 2016; **95**: 51-67.
55. Hof PR, Der Gucht EV. Structure of the cerebral cortex of the humpback whale, Megaptera novaeangliae (Cetacea, Mysticeti, Balaenopteridae), Anatom Rec, Part A: Discov Molecul Cellular Evolut Biol 2007; **290**(1): 1–31.
56. Gonçalves MS, Lopez RH, Miguel LFF. Search group algorithm: a new metaheuristic method for the optimization of truss structures, *Comput Struct* 2015, **153**: 165-84.
57. Miguel LFF, Lopez RH, Miguel LF. Multimodal size, shape, and topology optimisation of truss structures using the Firefly algorithm, *Adv Eng Softw* 2013; **56**: 23–37.
58. Kaveh A, Javadi SM. An efficient hybrid particle swarm strategy, ray optimizer, and harmony search algorithm for optimal design of truss structures, *Period Polytech Civil Eng* 2014; **58**(2): 155-71.
59. ASCE. ASCE/SEI 7-16 *Minimum Design Loads* For *Buildings* And *Other Structures*, in American Society of Civil Engineers, 2016.
60. CSI. Computers & Structures, Inc, CSI Analysis Reference Manual for SAP2000 Ver. 20, Walnut Creek, CA, 2017.